IMAGE FUV and in situ FAST particle observations of substorm aurorae

S. B. Mende, C. W. Carlson, H. U. Frey, and T. J. Immel
Space Sciences Laboratory, University of California, Berkeley, California, USA

J.-C. Gérard
L'Université de Liège, Belgium

Received 27 March 2002; revised 26 July 2002; accepted 16 August 2002; published 7 March 2003.

[1] Images from the IMAGE Wide-band Imaging Camera (WIC) and Spectrographic Imager (SI) channels SI-12 and SI-13 were compared to in situ data taken by FAST during several substorms. FAST spacecraft observations have shown that the high latitude auroral ionosphere has several distinct regions. Intense auroras are seen in regions of upward directed quasi static electric fields and of Alfven wave accelerated superthermal electrons. In two of the cases presented, the satellite passed through an active poleward propagating substorm surge on its duskward flank. Both show that the superthermal wave accelerated component to be on the polar cap boundary of the surge, and that it could be distinguished from quasi static field "inverted V" precipitation which occurred at the more equatorward parts of the auroral oval. In one of these cases, the surge was accompanied by intense ion outflow. Three cases showed the FAST satellite passing through the substorm aurora at midnight or the dawn side outside of the surge and the wave accelerated electrons were less clearly separated from the inverted V type precipitation. The wave accelerated electrons were seen to be part of very short-lived transient events, i.e., bursts. The region of auroral forms, associated with Alfven waves exhibit relatively soft auroral precipitation with very intense electron fluxes. By comparing the intensity of the WIC and SI-13 channels of IMAGE FUV, it is possible sometimes to distinguish optically between the two types of regions. Global imaging of the two regions would allow the separation of quasi-static plasma convection regions containing inverted V-s from regions of Alfven wave driven electrons signifying substorm related magnetic field dynamics. *INDEX TERMS:* 2704 Magnetospheric Physics: Auroral phenomena (2407); 2788 Magnetospheric Physics: Storms and substorms; 2716 Magnetospheric Physics: Energetic particles, precipitating; 2708 Magnetospheric Physics: Current systems (2409)

Citation: Mende, S. B., C. W. Carlson, H. U. Frey, T. J. Immel, and J.-C. Gérard, IMAGE FUV and in situ FAST particle observations of substorm aurorae, *J. Geophys. Res.*, *108*(A4), 8010, doi:10.1029/2002JA009413, 2003.

1. Introduction

[2] Auroral electron precipitation is most often produced by field aligned quasi-static electric fields that accelerate electrons into the atmosphere. These fields are usually characterized by their particle signatures, which have relatively sharp mono-energetic peaks with an enhanced low energy component attributed to backscattered secondaries [*Evans*, 1974]. From the appearance of the spectrograms taken along satellite tracks, these signatures of field aligned electric fields were termed "inverted V" events [*Frank and Ackerson*, 1971]. *Newell* [2000] pointed out that electron spectra exhibiting mono-energetic peaks seldom follow the inverted V model of electric fields which would produce the highest potential drop in the middle of the feature along the satellite orbit path. Newell points out that these features usually have the strongest acceleration near the edges and prefers to call these quasi-static potential structures "Large Scale Electron Acceleration Events" (LSEA). In this paper we will continue calling the quasi static field aligned electric field accelerated electron events [*Temerin et al.*, 1994] "inverted V-s", fully recognizing that the transverse non-field aligned structure of these usually can be highly variable and need not adhere to the "V" shape. In summary, these electron precipitation features manifest themselves as having relatively mono-energetic peaks with an enhanced low energy component attributed to backscattered secondaries. The electron pitch angle distribution in these events is relatively isotropic because the magnetic mirror forces between the acceleration region and the satellite tend to counteract the pitch angle change caused by the field aligned acceleration. The existence of electrons of a different spectral characteristic, the so-called superthermal electrons, has been known for some time. These superthermal, field aligned bursts are characterized by fairly broad spectral

0148-0227/03/2002JA009413$09.00

enhancement [*Johnstone and Winningham*, 1982] and are usually explained as electrons accelerated by wave particle interaction [*Burch*, 1991; *Temerin et al.*, 1994]. Superthermal bursts are highly collimated along the field line and although they were found in association with inverted V-s [*Burch*, 1991], they were also found on their own [*Johnstone and Winningham*, 1982; *Newell*, 2000]. Simultaneous occurrences of waves characterized as Alfven waves and superthermal electron bursts were seen in Freja satellite data [*Boehm et al.*, 1995; *Stasiewicz et al.*, 1997, 1998; *Gary et al.*, 1998; *Knudsen et al.*, 1998; *Wahlund et al.*, 1998].

[3] FAST spacecraft observations [*Carlson et al.*, 1998] have shown that the high latitude auroral ionosphere has several distinct regions. There is a downward current region containing diverging electric field structures, up going field aligned electrons, small scale density cavities, and B-perpendicular ion heating. This region, in general, is devoid of intense auroral precipitation. The second region is an upward current region containing converging electric field structures, large-scale density cavities, down-going inverted V electrons, and upgoing ion beams and conics. These two regions are generally consistent with quasi-static potential structures [*Ergun et al.*, 1998; *McFadden et al.*, 1999]. In the upward current region, intense auroral displays are present and the currents are carried mainly by downward moving precipitating electrons.

[4] A third distinct region, characterized by filamentary currents containing Alfvenic electric fields, field aligned counter streaming (superthermal) electrons, and ion heating transverse to B with associated large ion outflow, is also seen in the FAST data.

[5] The FAST observations of superthermal electrons are consistent with features of the accelerated electron component obtained by simulations of the inertial Alfven waves as they propagate through an altitude dependent density profile and explained through Landau resonance of the cold ionospheric and magnetosheath electrons [*Chaston et al.*, 2000]. Inertial Alfven waves propagating in regions of auroral electron acceleration span the entire altitude range of FAST observations (350–4180 km) [*Chaston et al.*, 2000]. The field structures are electron skin-depth sized and the waves are dispersive carrying an electric field component parallel to the geomagnetic field leading to the formation of magnetic field-aligned density cavities and electron acceleration [*Stasiewicz et al.*, 2000]. High resolution measurements show that the electron distribution inside the impulsive wave field envelope or density cavity consists of a cold ionospheric component and an accelerated and heated field-aligned component comprised of downgoing and reflected ionospheric electrons [*Chaston et al.*, 2000].

[6] Soft electron precipitation [*Chaston et al.*, 2001a, 2002] and ion outflows [*Tung et al.*, 2001] are strongly enhanced in the Alfvén wave dominated acceleration region, which is often observed near the polar cap boundary. In summary, the third region is characterized by electron precipitation with monotonically decreasing electron energy distribution with field-aligned beam-like pitch angle distribution. The FAST instrumentation is especially well suited to discriminate these regions through its ability to resolve the energy and pitch angle of the precipitating particles.

[7] In this paper we will show global images of substorms from the IMAGE spacecraft. In these images, substorms can be identified by the sudden intensification of the quiescent aurora at substorm onset, usually near midnight local time. The intensifications propagate poleward while expanding in local time both west- and eastward. Following this phase, the aurora generally stops expanding and slowly fades. We will examine several FAST satellite passes crossing the aurora at different local times and in different phases of the substorm as defined by the global images.

[8] An example of a prior study, where global satellite images were not available, *Lopez et al.* [1991] presented southern hemisphere particle electron and ion spectrogram from a DMSP F7 pass. Using northern hemisphere magnetic data, they concluded that a substorm was occurring at the conjugate region. Magnetic activity was recorded about 1 hour prior to the satellite pass at mid- and high-atitude northern stations. Equatorward, the DMSP particle spectrogram showed a region of diffuse electron precipitation with a narrow discrete embedded feature. As the DMSP satellite moved poleward it encountered a broad region of mono-energetic (12 keV) electrons. Continuing poleward, there was a region of highly structured discrete precipitation that was quite different from the unstructured region both in spectral and spatial characteristics. This was observed near the boundary of the polar cap. The spacecraft magnetometer data also showed that the largest field aligned current was coincident with the region of highly structured energetic electron precipitation. *Lopez et al.* [1991] state that the DMSP imagery did not help because the highly disturbed nature of the aurora in the DMSP images makes the unambiguous identification of any specific surge feature problematic. Their determination of substorm onset in UT and MLT was also questionable without simultaneous global auroral image sequence. In addition, their assumption of perfect hemispheric conjugacy of substorm features does not always hold true [*Frey et al.*, 1999]. In the case discussed by *Lopez et al.* [1991] it is possible that the bulk of the field-aligned current is produced by the large, spatially diffuse, regions containing the mono-energetic (inverted V) precipitation, however the optical surge itself is generally the most intense poleward and westward edge of the auroral region. It was probably located in the region described by *Lopez et al.* [1991] as highly structured discrete precipitation.

[9] On the IMAGE spacecraft an extensive instrument complement was flown to observe the global aurora in the far ultraviolet (FUV). The instrumentation consists of the Wideband Imaging Camera (WIC) and the Spectrographic Imager (SI). WIC observes the aurora in a broad band (140–170 nm), sensitive mainly to LBH N_2 and some NI lines. The SI-12 channel, one of the two channel of the Spectrographic Imager (SI), images Doppler shifted Lyman alpha to monitor the global scale proton precipitation [*Mende et al.*, 2000] by suppressing the intense (>10kR) geocoronal Lyman alpha background, which would otherwise appear as an impenetrable diffuse background glow. The third channel, the SI-13 channel, has a 5 nm wide band (full width at half maximum) centered on the auroral OI 135.6 nm line. In addition to this line, there are two components of LBH, which also contribute to this passband. The auroral emissions in this band are absorbed to a greater degree by molecular O_2 than the emissions sensed by the WIC instrument. The intercomparison of the intensity of the

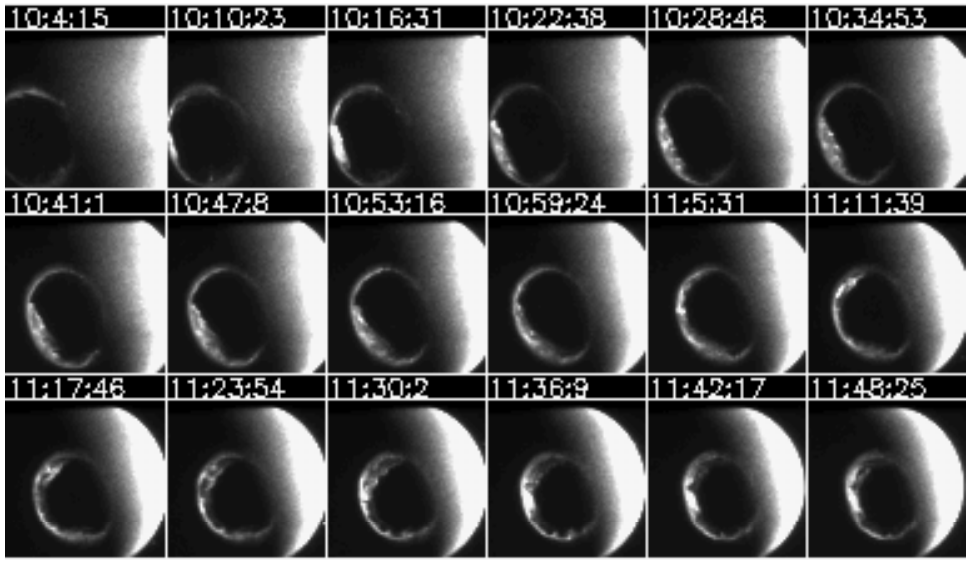

Figure 1. Collage of WIC images to depict the auroral development preceding the October 28, 2000 FAST pass (orbit 16608). In the first few images the clock angle of the noon midnight meridian is about 2:30.

signal in the SI-13 and WIC channels during auroral observation can provide information about the mean energy of the precipitating particles. For instance, large SI-13 to WIC intensity ratios signify soft electron precipitation [*Hubert et al.*, 2002]. The responsivities of these instruments was validated by laboratory and in-flight calibrations using auroral observation with simultaneous in situ FAST and DMSP spacecraft-based electron and ion flux measurements [*Frey et al.*, 2001; *Gérard et al.*, 2001]. The high spatial resolution and dynamic range, and the ability to distinguish proton precipitation allows us to examine the relative importance of the space-time morphology of the auroral regions containing inverted V-s and Alfven wave accelerated super-thermal electron precipitation as observed simultaneously by the in situ instrumentation on the FAST satellite. This study will help us in assessing the relative importance of two types of auroral acceleration mechanisms which are part of the substorm process. We will discuss 5 passes of the FAST satellite through the northern nightside auroral oval when simultaneous images were acquired by the IMAGE spacecraft and the auroral oval was in a high state of activity due to a substorm preceding the period.

2. Data Presentation

[10] For each event the FUV images are presented in the form of a collage. The first collage is an overview to provide the most significant WIC images representing the development of the auroral substorm preceding the FAST satellite pass. Then we present a second collage of every image available during the FAST satellite pass to show the details of the aurora during the actual pass. The WIC images, presented in a red temperature scale, are representative of the auroral and dayglow LBH N_2 and N emissions. For some cases, we present the SI-12 image (blue) showing proton induced Lyman alpha [*Mende et al.*, 2000] and the SI-13 (green) showing the 135.6 nm contribution. Dayglow was removed from the raw WIC images by subtracting a 40 pixel Gaussian smoothed version of the image. The subtraction removed the slowly varying large-intensity dayglow thus allowing the presentation of fine scale aurora in the sunlit and dark regions. Without this correction the dynamic range spanned 14 bits and would have been impossible to display on any viewing device or in print. The SI-12 instrument responds only to Doppler shifted Lyman alpha emissions produced by charge exchanged protons [*Mende et al.*, 2000; *Frey et al.*, 2001]. Laboratory calibrations showed that SI-12 channel of the Spectrographic Imager responds to red shifted Lyman-α radiation only at wavelengths greater than 121.7 nm. It is unlikely that auroral protons of less than $\sim$1 keV of primary energy would produce appreciable emission at these wavelengths [*Gérard et al.*, 2001]. Thus we do not expect that the instrument would respond to protons of primary energy less than 1 keV. The third, the SI-13 channel, is primarily responsive to soft electrons. Hard auroras penetrate deep into the atmosphere and the atmospheric O_2 absorbs most of the emissions that are produced further down in the atmosphere. Geomagnetic latitude (45, 60, 75 and 90) and magnetic local time (midnight, 0300, 0600, 0900, 1500, 1800, 2100) were superimposed with solid lines on all the images presented in Figures 2, 5, 8, 11, and 14. Magnetic noon was indicated with a dashed line. The position of the FAST satellite is indicated by a small box with a short segment of the orbit track in the middle.

[11] The FAST satellite data is presented in a time series data format. Panel 1 and 2 show the parallel and perpendicular pitch angle electrons. Panels 3 and 4 are the electron energy flux and number flux, respectively. Panel 5 is the parallel ion spectrogram and panels 6 and 7 are the ion energy and number fluxes, respectively. Note that in all the flux data the net direction up or down are represented with colors red and green, respectively. Panels 8, 9 and 10 represent the IMAGE FUV optical observations under the mapped satellite track. These data were extracted from the

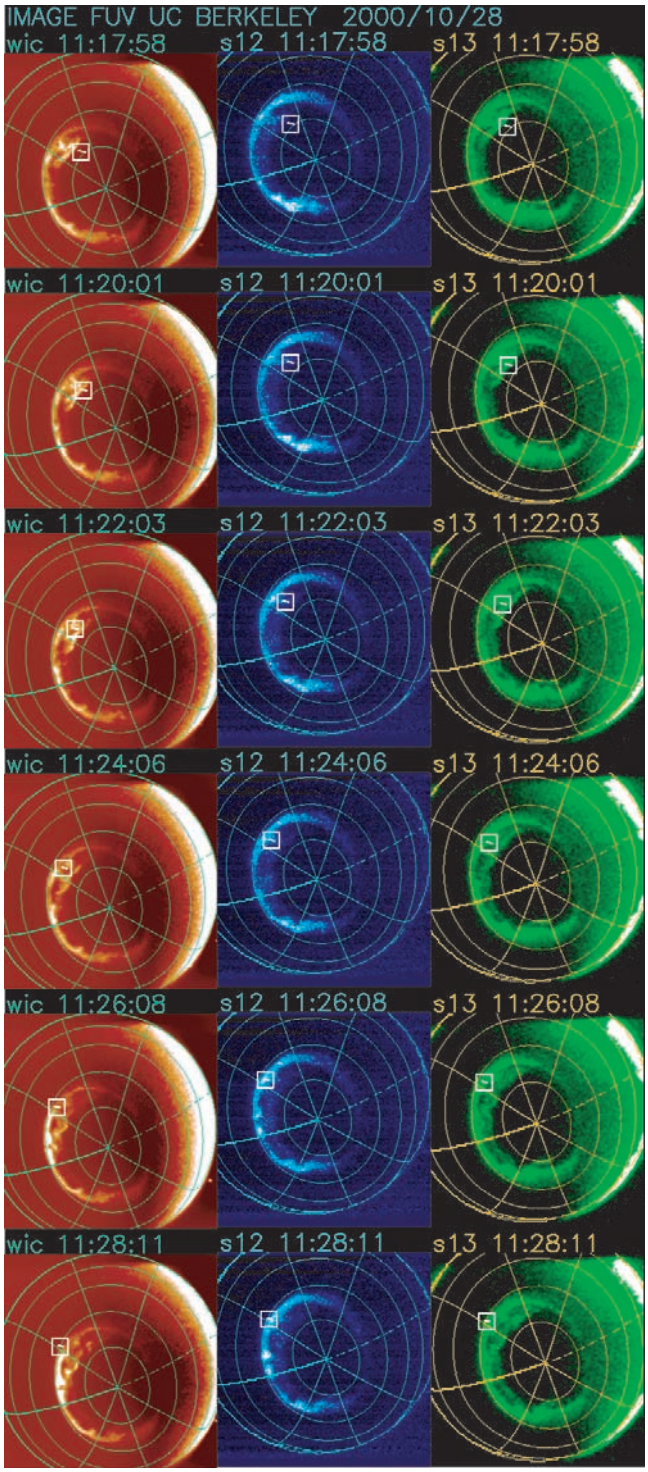

Figure 2. Collage of the WIC, SI-12 and SI-13 images for the FAST pass on October 28th, 2000 (orbit 16608).

images taken at the time nearest to the time indicated on the spectrogram. They are in raw A/D units for WIC and photoelectron counts per pixel per exposure for SI-12 and SI-13. IMAGE orbit is highly elliptic with perigee at 1000 km (south) and apogee 44,000 km (north). The observing situation is best when IMAGE is closer to the aurora than at apogee. This criterion seriously limits the number of cases available for this type of analysis.

2.1. October 28, 2000

[12] Magnetic field quick look data from the WIND satellite (X = 48, Y = −156, Z = 90, solar magnetospheric coordinates) for the period of interest (day 302, 11–12 UT) show that the IMF B_y component was negative (−5 nT) and gradually increasing toward zero. The AL index starts turning downward just before 1000 UT with a very sharp downturn at about 1020 UT. There is a sudden increase in the solar wind pressure at 09:30 and an increase of the solar wind velocity from 350 to 450 km/s. IMAGE FUV data sequence covering the period preceding the FAST pass between 1004 and 1124 Oct 28, 2000 (302) is shown on Figure 1.

[13] At the start of the sequence (1004), a substorm is presumably already in progress, except that it is out of the field of view. We observe the substorm in the first image at 1010 and follow its poleward and eastward expansion until 1035. The surge fades significantly by 1105. At 1111 on the dusk side of the auroral oval, a new active surge commences, spreading poleward and expanding simultaneously in the dawn and dusk directions. The FAST satellite passes through this newly developed surge region at 1117, or 6 minutes after the start of the surge. Some substorm features described by *Mende et al.* [2001] can be seen in this event. For example, the temporal and spatial coincidence of the initial proton intensification and poleward expansion with the electron auroras (not shown). Shortly after that, intense electron aurora dominates the high latitude edge of the expansion surge. It is also worth noting that at the onset of the first expansion, the protons behave similarly to the electrons and both electrons and protons spread evenly in local time from the region of the initial brightening.

[14] The relevant images (WIC, SI-12, and SI-13) to the FAST nightside orbital crossing are shown in Figure 2. The satellite is still in the polar cap at 11:17, it reaches the electron surge (WIC and SI-13) at 11:20, it crosses the densest region of the proton precipitation at 11:26 and emerges on the equatorward side of the oval. The FAST positions are illustrated on Figure 2 as small square boxes.

[15] The FAST particle data and the IMAGE luminosity plots along the orbit track are shown on Figure 3. The total precipitated electron energy (3rd panel) shows a strong enhancement at 1120 in agreement with the position of the surge on the images. There are actually two narrow peaks in the electron fluxes, reaching several tens of ergs cm^{-2} s^{-1} (mWm^{-2}), but their spatial widths are less than the resolution of the imagers. These are coincident with the enhancements in the WIC and SI-13 data (panel 8 and 10). The precipitated ion energy plot shows a broad peak at 61° ILAT, (11:27:20 UT) reaching about 1 erg cm^{-2} s^{-1}. The electron spectrogram shows that the large precipitated intensity peaks associated with the surge have strong super-thermal components and the pitch angles are highly field aligned. These spectra are generally characteristic of wave produced acceleration. Just equatorward of these features, approximately at 11:21, we see two small spectral features which have very similar appearance in both the parallel (panel 1) and in the perpendicular (panel 2) components, showing that they are inverted V type precipitation. The rest of the auroral oval between 11:22 and 11:27 shows the spectra of less intense precipitation with a broad peak at a few keV that generally have the character of an inverted V.

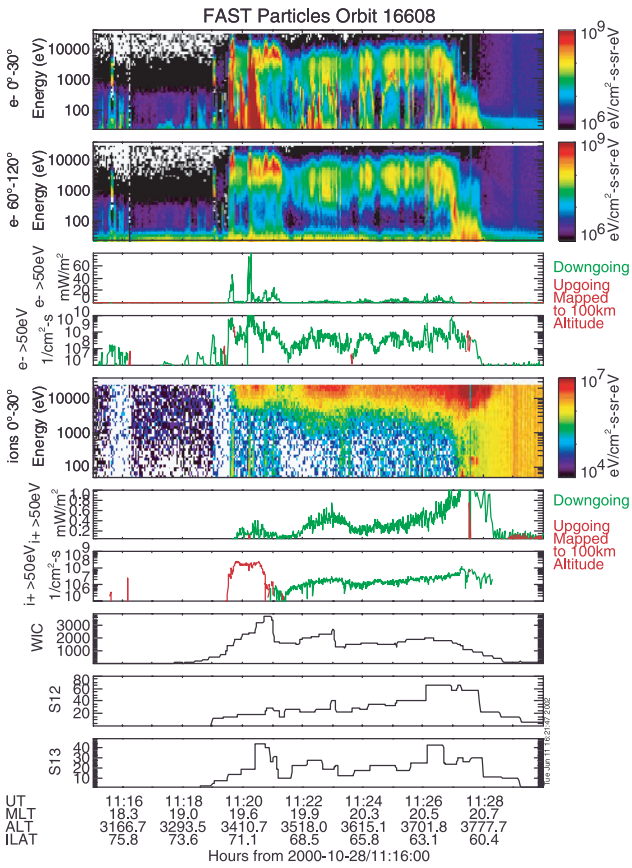

Figure 3. FAST and IMAGE data, spectrogram of downward (0°–30° pitch angle) electrons (panel 1), mirroring (60°–120° pitch angle) electrons (panel 2), electron energy flux (panel 3) and electron number flux (panel 4), ion energy spectrogram of downward (0° – 30° pitch angle) ions (panel 5), ion energy flux (panel 6), ion number flux (panel 7), IMAGE WIC A–D units (panel 8), IMAGE Spectrographic Imager SI-12 and SI-13 counts (panels 9 and 10). On the flux plots panels 3, 4, 6, and 7 green is net downward flux and red is upward flux.

The ion spectrograms are considerably less structured showing a monotonically decreasing spectrum with latitude on the upper side of the energy scales of the FAST instrumentation. The upper boundary and perhaps even the mean of the energy of precipitation is above the energy range (<25 keV) of the ion detectors on FAST. It should be noted that there are energetic precipitating protons (panel 5) at the location of the surge. However, the energy flux carried by these protons is below the detection threshold of the IMAGE SI-12 instrument. The FAST ion energy flux data (panel 6) and the IMAGE SI-12 data (panel 9) show relatively good qualitative agreement. Quantitatively, however, the SI-12 counts imply about 2–3 erg cm^{-2} s^{-1} [*Gérard et al.*, 2001] compared to 1 erg cm^{-2} s^{-1} measured by FAST. The discrepancy is believed to be due to protons above the energy threshold of the proton detectors and believed to be of plasma sheet origin. From 11:22 to 11:28 a slight lowering of the boundary of the ion energy range with increasing latitude can be seen. Another remarkable feature of the FAST data is the strong ion outflow shown by the ion flux plots (panel 7) depicting an outflow (red color) of 10^8 ions cm^{-2} s^{-1}at the position of the surge.

[16] The bottom panels 8 and 10 show the IMAGE data in "counts" per pixel per exposure for WIC and SI-13. A distinct peak is seen just before 11:21. Using the IMAGE calibration data, these are interpreted as a mean energy of 4.3 keV, energy flux of 13 mW/m^{-2} and an electron flux of 2×10^9 cm^{-2} s^{-1} [*Hubert et al.*, 2002]. This is in fairly good agreement with the FAST data when it is averaged over the relatively coarse spatial resolution element of IMAGE FUV.

[17] In summary, on October 28, 2000 FAST flew into an active expanding surge. The electrons in the surge showed the superthermal energy and the beam-like pitch angle distribution characteristic of the Alfven wave accelerated particles. The ions, after a brief poleward excursion, were present only equatorward of the surge with no enhancement poleward of their normal auroral oval position. The surge was accompanied by intense ion outflow which reached about 1 keV in energy at the FAST satellite. IMAGE FUV was able to put the in situ measurements in context with the global development of the surge and the rest of the auroral oval.

2.2. January 19th, 2002

[18] WIND (x = 33, z = 0 solar magnetospheric) shows that B_z is largely positive but around 1315 a short pulse of negative B_z is seen lasting about 10 minutes. The solar wind V_x rises from 320 to 350 km sec at 1310 and was accompanied by an ion dynamic pressure pulse reaching 5 nPa. The AL index shows a sharp onset at 1250. From the IMAGE overview plots (Figure 4) one can recognize that the substorm onset was at about 12:49. There is a small poleward expansion which is discernable at 13:51:15 at the bottom of the frame. The FAST satellite went through this region at 13:53.

[19] The IMAGE FUV data corresponding to the FAST pass is shown on Figure 5 and the FAST data on Figure 6. In Figure 5, we can see that the satellite encounters a small poleward surge feature that contains a moderate flux of protons because it produces a significant signal in the SI-12 channel at 13:49. During the satellite pass the protons become much fainter as the electron aurora continues its expansion. The aurora is best seen in the SI-13 channel. As FAST emerges from the polar cap we can see a sudden rise in the precipitated electron energy flux to 20 ergs cm^{-2} sec^{-1} at 1352:30 (panel 3 Figure 6). The electron spectrograms (panel 1 and 2) show that most of the electrons are superthermal with a beam like pitch angle distribution. A moderately intense inverted V precipitation feature is observed around 1355. Moderate intensity ion precipitation is also seen poleward of this feature. The ion spectrogram (panel 5) at 1353 seems to indicate highly energetic particles with the mean energy probably beyond the energy bandpass of the instrument. According to the energy flux plot (panel 6) the strongest feature may be seen at 1355 although again the bulk of the ions could be above the energy range of the instrument.

[20] As FAST travels equatorward from the polar cap, there is a discernable enhancement that develops on the poleward edge of the electron and proton oval. It is quite clearly visible on frames 1351 in WIC and SI-12. This is the

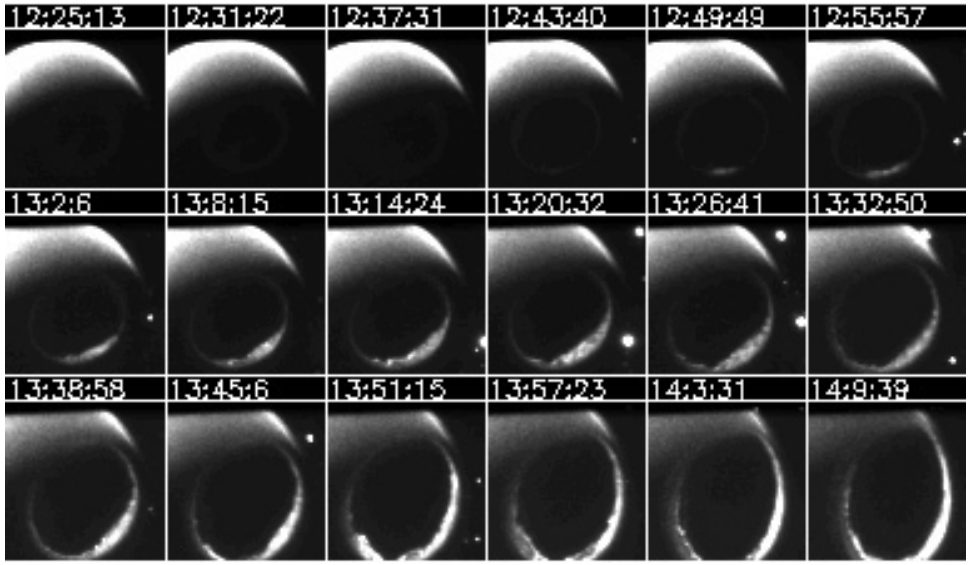

Figure 4. Collage of the WIC images from substorm onset to the FAST pass for January 19th, 2002 for FAST orbit 21545.

feature that the satellite passes at 1353. The main part of the electron oval was passed at 1355 simultaneously with the brightest region in the ions. These images are in very good agreement with the location of FAST in situ measurements. The poleward part of the auroral region was caused by superthermal electrons which were presumably accelerated by waves. This region extends equatorwards reaching 64 degrees latitude. Below this there is a region of inverted V precipitation with a mean energy of about 3–4 keV. Comparing the FAST data panel 3 (electrons energy flux) and panel 6 (ion energy flux), the strongest peak of the ion precipitation was collocated with the electrons on the equatorward side of the oval where the electron spectrogram registered an inverted V potential structure. The FAST data show that the narrow poleward edge of the surge arc was more intense than the aurora anywhere in the rest of the oval. The surge aurora should be $\sim$ 50 km in width according to the FAST electron data which is smaller than the spatial resolution of the imager. Therefore, the apparent intensity of the image is reduced. We can see that at the poleward part of the aurora the SI-13 to WIC ratio (panel 10 to panel 8) is larger than at the equatorward part showing that the Alfven wave accelerated superthermal electrons are of lower energy than those produced by the inverted V acceleration mechanism. In summary, the satellite passed through an expanding surge consisting of Alfven wave accelerated superthermal electrons and of energetic protons. The rest of the oval consisted of intense fluxes of electrons produced by inverted V potential structures.

2.3. May 12, 2001 1930

[21] Two substorms occurred on May 12, 2001 when IMAGE and FAST were favorably located to look at post substorm auroras. WIND (X = 27.5, Y = – 200, Z = – 25, solar magnetospheric coordinates) magnetic field data show that during the period of interest (day 132, 19–20 UT) the IMF B_z component was zero, however it had briefly gone to 7 nT positive at 18:40 and then suddenly to –5 nT for a brief interval returning to zero by 19:00. The substorm onset at 19:09 could be a response to this fluctuation (Solar wind speed = 650 km/sec). The AL index shows a very sharp downturn (1000 nT) at about 19:25 UT and another (700 nT) at about 21:20 UT. This latter period will be discussed separately as the next event.

[22] IMAGE FUV WIC data covering the period preceding the FAST pass between 1851 and 1958 May 12, 2001 (132) is shown on Figure 7. The FAST pass occurs near 1930.

[23] At the start of the sequence (1851) there is very little activity at midnight. A little later, at 1909 some activity is clearly seen at midnight. The most intense part of the activity is on the dusk sector however there is a rapid motion toward dawn and poleward post midnight.

[24] The relevant images coincident with the FAST pass are shown on Figure 8. The satellite is still in the polar cap at 19:20, reaching the electron surge (WIC) in the image at 19:22:10, crossing the densest region of precipitation at 19:24 to emerge on the equatorward side of the oval by 19:36 UT. The FAST particle data is shown on Figure 9. The total precipitated electron energy flux (panel 3) shows enhancements at 19:22 and 19:23. Although the two narrow peaks in the electron energy flux reach about 8–10 ergs cm^{-2} s^{-1} their spatial width is less than the resolution of the imagers. The ion precipitated energy plot (panel 6) shows a broad region of precipitation from 19:24 to 19:35 (70° ILAT to 56° ILAT) averaging 0.1 erg cm^{-2} s^{-1}. The electron spectrogram shows that the largest precipitated intensity peaks associated with the surge have strong super thermal components and the pitch angles are highly field-aligned at the poleward edge of the aurora. These spectra are generally characteristic of wave produced acceleration. From around 19:23 and later (to 19:35), all the spectrogram features have relatively similar appearance in the parallel (panel 1) and in the perpendicular (panel 2) components showing that they are of isotropic pitch angle. The ion spectrograms are less structured showing a monotonically decreasing energy trend with latitude. The upper boundary of the energy of precipitation is above the range of the ion detectors on FAST.

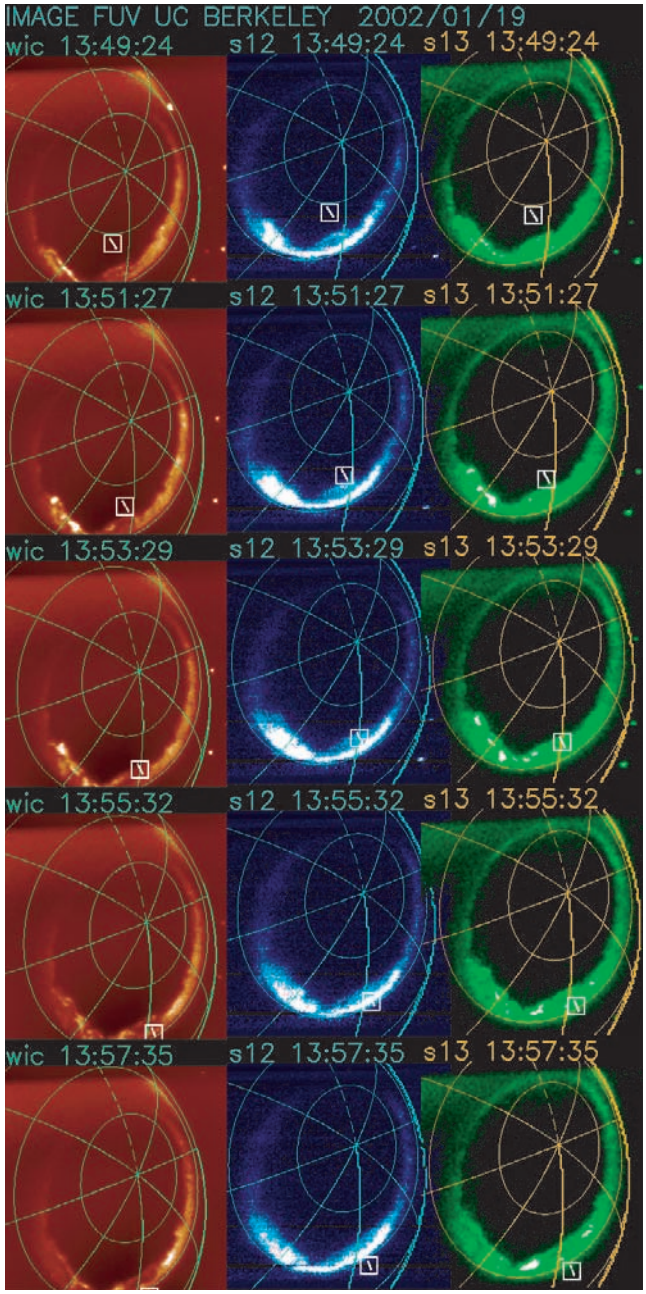

Figure 5. Collage of the WIC, SI-12 and SI-13 images for the FAST pass on 19th of January 2002 for FAST orbit 21545.

[25] Summarizing the May 12, 2001 event, FAST flew into an expanding surge about 10 minutes after the substorm onset. It appears that the satellite flew across the eastern end of the surge missing its most intense part. Nevertheless the satellite saw a precipitated energy peak consisting of super-thermal electrons with the beam like pitch angle distribution characteristic of Alfven wave accelerated particles. The rest of the electron precipitation in the very wide oval consisted of inverted V type electrons.

2.4. May 12, 2001, 2135

[26] WIND (X = 27.5, Y = – 200, Z = – 25, solar magnetospheric coordinates) magnetic field quick look data shows that during the period of interest (day 132, 20–22 UT) the IMF B_z component was zero. As mentioned before, the AL index shows a very sharp downturn (700 nT) at about 21:49 UT. IMAGE FUV data sequence covering the period preceding the FAST pass between 21:18 and 21:49 May 12, 2001 (132) is shown on Figure 10.

[27] At the start of the sequence (21:18) there is very little activity at midnight. At 21:43 two hot spots develop one at pre-midnight (21:24) and one post midnight. By 21:30 the expansion is in full force. The most intense part of the activity is on the dusk sector, however the entire nightside aurora expands poleward pre- and post-midnight 21:30. The FAST pass occurs between 21:33 and 21:45 UT.

[28] The relevant WIC images to the FAST nightside orbital crossing are shown on Figure 11. The satellite is still in the polar cap at 21:33, reaches the electron surge in the image at 21:35:09, to emerge on the equatorward side of the oval by 21:43 UT. The FAST positions are illustrated on Figure 11 as small square boxes. The FAST particle data is shown on Figure 12. The total precipitated electron energy shows enhancements at 21:36:10 and 21:37. The two narrow peaks in the electrons reach about > 100 ergs cm^{-2} s^{-1}. Their spatial width is less than the resolution of the imagers. The electron spectrogram shows that the large intensity peak at the poleward side of the surge (21:36:10) has a strong super-thermal component and its pitch angle distribution is highly field aligned. These spectra are generally characteristic of wave produced acceleration. The

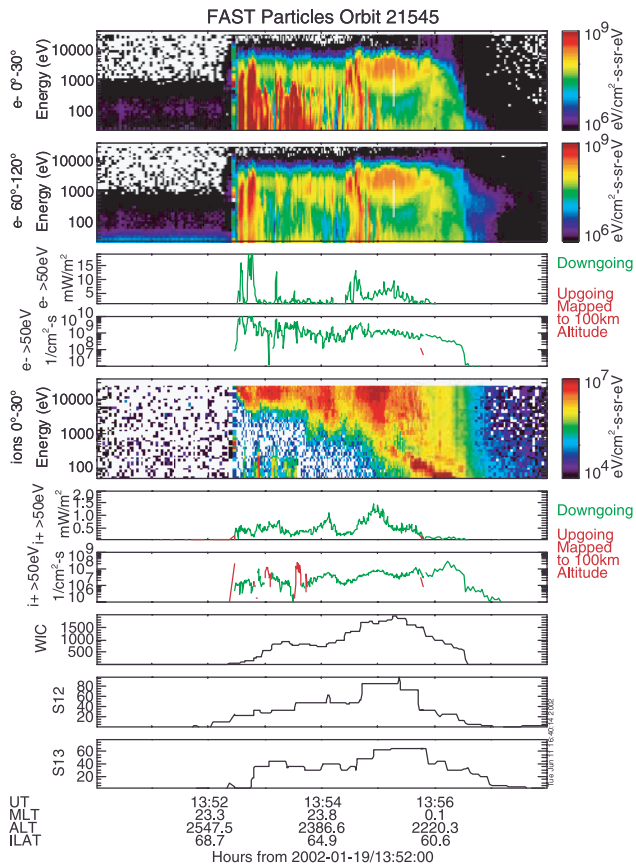

Figure 6. FAST electron data for the outbound orbit number 21545 (same as Figure 3).

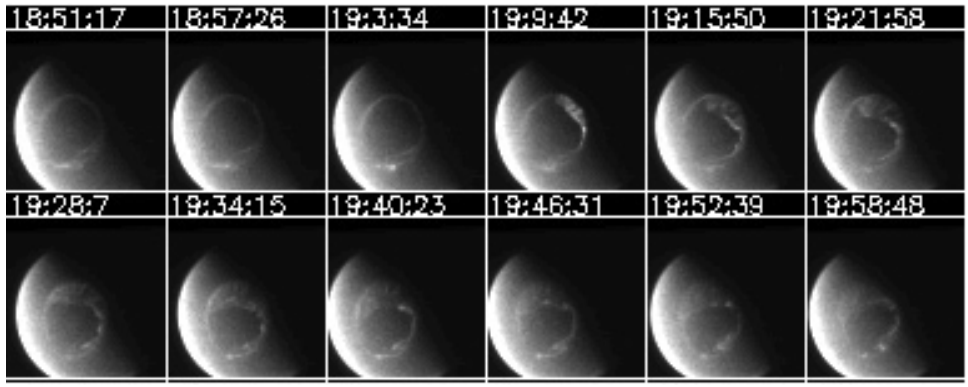

Figure 7. The auroral images prior to the FAST satellite pass. A small substorm onset occurred between 19:03 and 19:09 and the FAST overpass commenced at 19:20 however the main activity occurred a little west of the satellite track.

adjacent peak at 21:37 has a continuation of some intense low energy field aligned fluxes. However, it has a considerable component in the pitch angle range perpendicular to B that seem to consist of a separate group of higher energy >3 keV electron. Thus the components of this second peak cannot be regarded as having only wave accelerated electrons. It is possible that the currents, which are set up by the wave accelerated precipitating particles, become so intense that they produce a B parallel potential drop. The other weaker features equatorward (later than 21:37:40) do not show the enhanced low energy field aligned character of the superthermal electrons and are likely to be caused purely by inverted V type field structures. The ion spectrograms are considerably less interesting, showing that at the position of the electron aurora the mean energy of the precipitation is likely to be outside of range of the ion detectors on FAST (<25 keV).

[29] At the time of transiting the poleward part of the surge (~74° IL) the most intense part of the surge was west

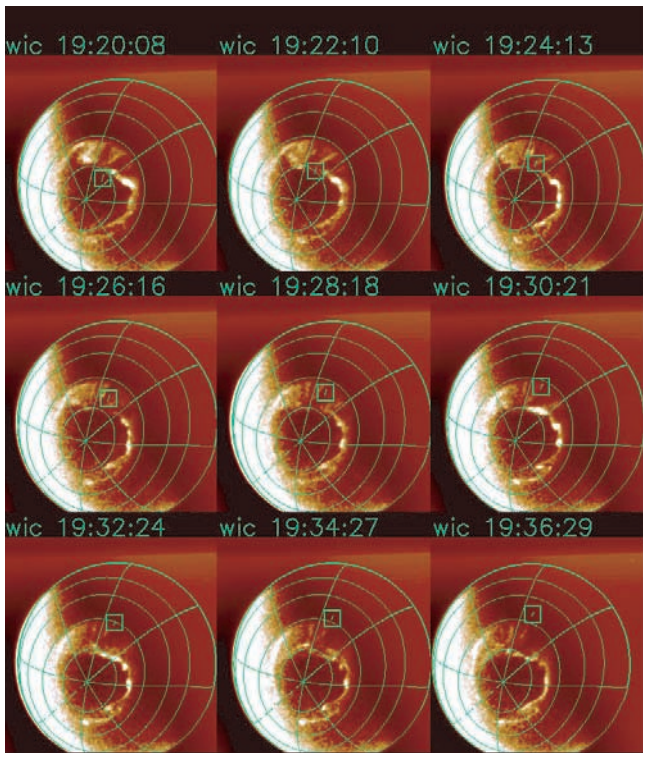

Figure 8. Collage of the WIC images for the FAST pass on 12th of May 2001 (orbit 18766).

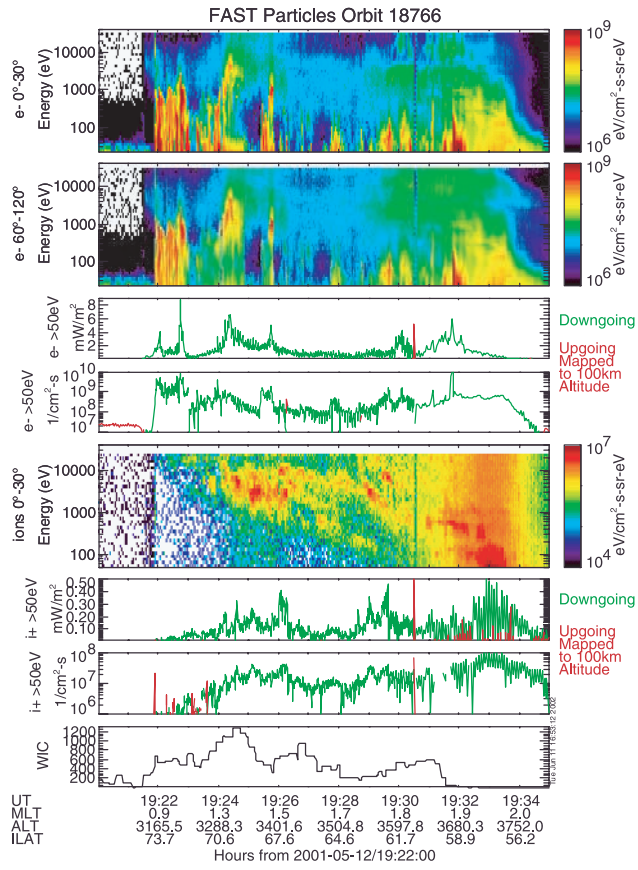

Figure 9. FAST particle data for the orbit number 18766. (Same as Figure 3 except that only IMAGE WIC is displayed as panel 8.)

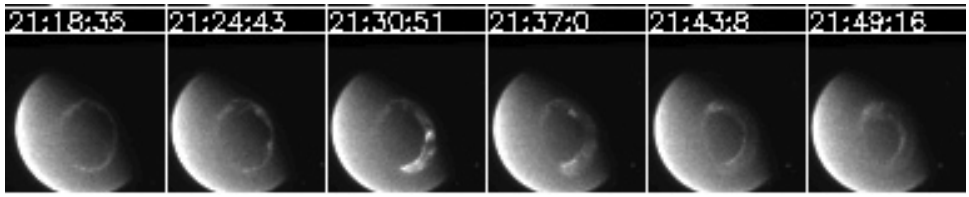

Figure 10. The auroral images prior to the FAST satellite pass. A small substorm onset occurred between 21:18 and 21:24 and the FAST overpass commenced at 21:35.

of the satellite (Figure 11, 21:35:09). In the image 21:37:12 FAST has just passed a very intense auroral feature which we identified in the spectrograms as a wave accelerated precipitation near the poleward boundary of the aurora. It is most interesting that this feature was only seen in the image taken at 21:37:12 and was not present at 21:35:09 or at 21:39:14.

[30] During the May 12, 2001 21:36 event FAST flew into an expanding surge about 10 minutes after the substorm started. It appears that the satellite flew across the eastern part of the surge missing the most intense westward part. It has encountered an intense, apparently wave accelerated electron peak. From the images, it was evident that this peak was a very short-lived feature lasting for less than 4 minutes.

2.5. June 11, 2000

[31] During this event WIND (X = 6R_e, Y = – 33 R_e, Z = – 4 R_e solar magnetospheric coordinates) magnetic field data show that during the period of interest the IMF_z component was weakly negative with a strong positive y component. The GOES 10 geo-synchronous satellite magnetometer data (provided courtesy of H. Singer) showed sudden dipolarization occurring at 1445 UT indicating that the data sequence started in the expansive phase of a substorm.

[32] The situation in Figure 13 is characteristic of the latter part of a substorm expansive phase followed by the recovery phase and leading to a "double auroral oval" [*Elphinstone et al.*, 1995a, 1995b]. The first images of the IMAGE data sequence (14:52) show a significant part of the nightside auroral oval. After 15:04 the surge faded and the above mentioned double oval configuration is seen by WIC consisting of a poleward region of discrete poleward auroras and a second more diffuse equatorward oval. The image sequence coincident with the pass is illustrated in Figure 14 where the WIC and SI-12 images are shown side by side. The FAST

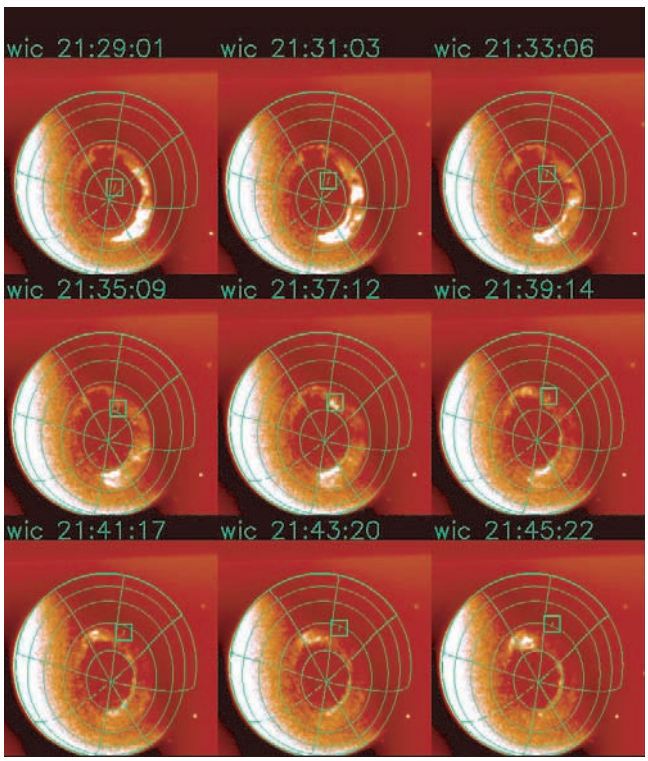

Figure 11. Collage of the WIC and SI-12 images for the FAST pass on 12th of May 2001 (orbit 18767).

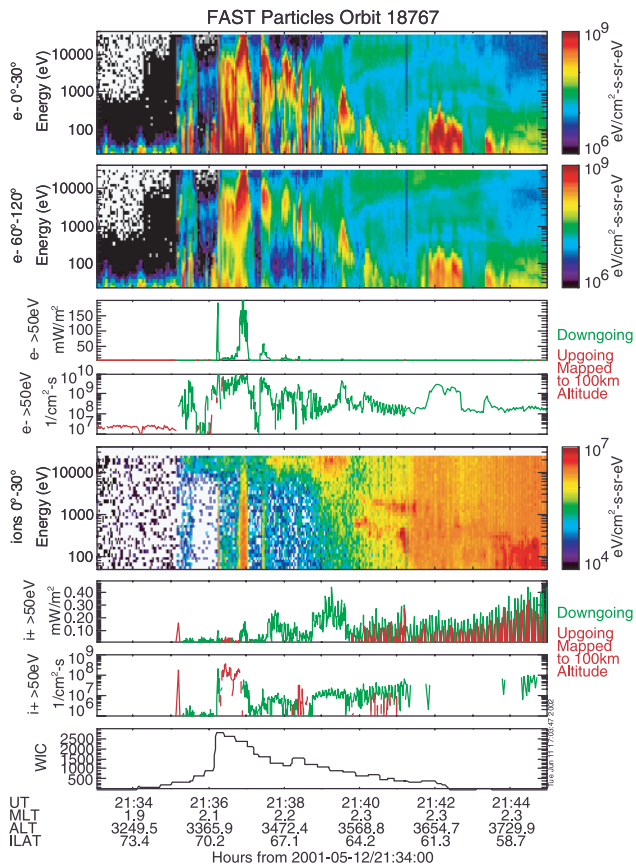

Figure 12. FAST particle data for the orbit number 18767. (Same as Figure 3 except that only IMAGE WIC is displayed as panel 8.)

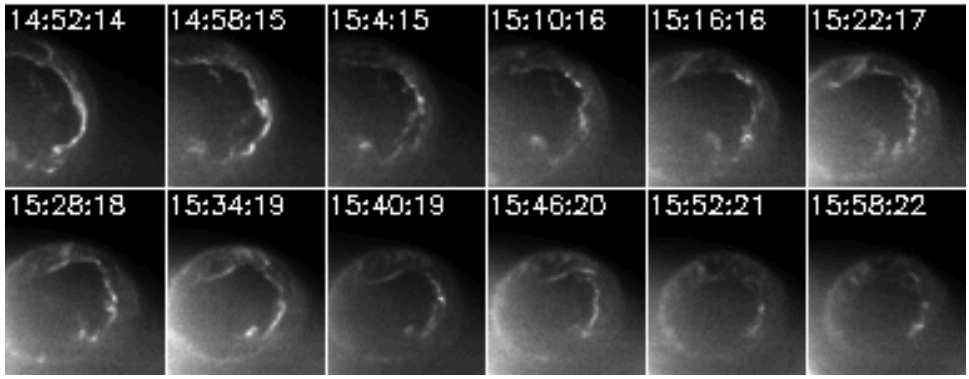

Figure 13. The auroral images prior to and during the FAST satellite pass commencing at 15:32 on June 11th, 2000.

data is shown on Figure 15. The proton aurora is seen (middle blue-white images), collocated with the diffuse region seen by WIC. There is a bright patch near midnight which is just equatorward of the substorm surge and presumably located at the substorm onset location [*Mende et al.*, 2001]. The duskward, more intense proton precipitation is longitudinally coincident with the vestiges of the substorm surge, but located equatorward of it. The intensity of the protons also faded with the auroras, that had been previously part of the substorm surge. After 1530 UT the proton auroras were located in the equatorward diffuse aurora.

[33] Between 1530 and 1538 the FAST satellite traversed the midnight auroral oval as illustrated by the small box and a three-minute track (one minute prior to the image time and two minutes following). The WIC and SI-13 images at 15:36:30 and 15:38:31 are almost identical to the recovery phase double oval situation described by *Elphinstone et al.* [1995a] in their Figure 1 top panel.

[34] The FAST electron spectrogram of downward electrons (Figure 15, 1st and 2nd panel) shows diffuse electron precipitation with embedded structures below latitudes of 67° ILAT (15:35 UT). The structures are either mono-energetic peaks (15:33:20, 15:34:40 and 15:35:10 UT) with high fluxes in both B parallel and perpendicular detectors consistent with isotropic pitch angle distribution or beams with monotonically decreasing energy spectra (15:33:15 and 15:37:10 UT). The most remarkable feature is the one at 15:33:15 which represents a particularly intense current sheet and large fluxes of precipitation. In this range, the electric field wave data (not shown) has amplitude greater than 100 mV/m and the phasing is consistent with a propagating Alfven wave. These observations are consistent with Alfven wave accelerated particles. The downward current region [*Carlson et al.*, 1998] coincides with a region of no electron precipitation between 15:35:10 and 15:36:00. Poleward of the gap, there is a large flux of 5 to 10 keV electrons also exhibiting mono-energetic peaks with enhancements at low energy due to reflected secondary electrons. This is typical of inverted V electron distribution produced by a quasi-static DC parallel electric field. At 15:37:10 there is another less intense batch of electrons with lower mean energy characteristic of Alfvenic wave accelerated electron distribution.

[35] Figure 15 panel 5 shows the downward ions (pitch angle = 0°–30°) energy spectra and total energy (panel 6) and flux (panel 7). At lower latitudes, the protons have significant fluxes and they are visible by the imager e.g., the SI12 data (panel 9). The electron energy flux (panel 3) shows a significant peak, of 30–40 erg cm^{-2} s^{-1} at 15:33:15 due to the Alfvenic feature. There is a strong response of the SI-13 (panel 10) signifying large flux of low energy electrons. The same type auroras are seen at 15:36 and 15:37 in the region of the poleward mono-energetic inverted V structures. In the most poleward Alfvenic structure, seen at 15:37:10, the energy flux is of the order of only 1 erg cm^{-2} s^{-1}. The proton energy flux (panel 6) peaks at lower latitude reaching an energy flux of 1 erg cm^{-2} s^{-1}.

[36] In the 15:32:30 image (Figure 14) the satellite is about to traverse a bright feature which is presumably the electron precipitation seen on the FAST plot at 15:33:15. In the 15:34:30 image, the satellite is poleward of the bright feature that seems to have also moved westward and became much weaker at the point of the FAST satellite transit. The FAST proton data also shows that at this time the satellite is at the poleward edge of the proton aurora. The 15:36:30 WIC image shows that FAST should be on top of a bright feature. This is precisely the time when FAST sees the bright poleward inverted V feature. In the next image (15:38:31), the satellite is already in the polar cap. The bright feature, which was seen by FAST at 15:36:30, is substantially diminished in the 15:38:31 WIC image.

[37] If we assume that inverted V type auroras are the signature of steady state convection boundaries and Alfven wave accelerated auroras are of substorm related magnetic field dynamics, then the relative weakness of this type of aurora compared to the inverted V aurora signifies the late phase of the substorm recovery. Our optical observations show that the poleward bright auroral feature, which contains these auroral types, is very dynamic.

[38] Most of the WIC images presented in Figure 14 show a double oval configuration with an equatorward diffuse region, a bright poleward edge separated by a darker band. Although the images usually show dynamic behavior, some of these images look very similar to a typical double oval drawn by *Elphinstone et al.* [1995a].

3. Discussion

[39] The high spatial resolution, dynamic range and the ability to distinguish proton precipitation of the IMAGE

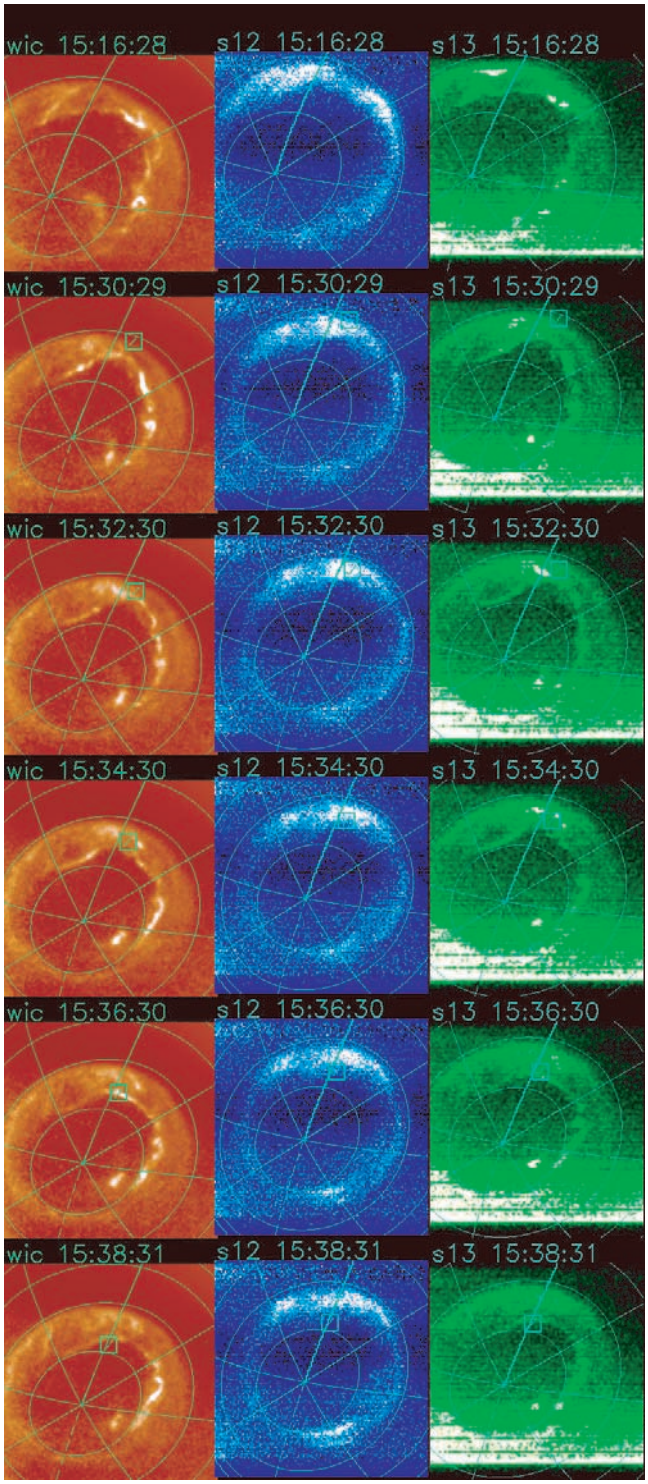

Figure 14. WIC SI-12 and SI-13 images during the fast pass of orbit 15088. Geomagnetic coordinates. Midnight meridian is thicker.

FUV instrumentation allowed us to examine the relative importance of the space-time morphology of auroral regions containing inverted V-s and Alfven wave accelerated superthermal electron precipitation. The high time, and pitch angle resolution capabilities of FAST are needed to clearly distinguish the different types of auroral mechanisms from each other.

[40] The examination of the IMAGE data coincident with several simultaneous FAST passes showed that the FAST electron spectrum is usually consistent with precipitation by field-aligned quasi-static electric fields or so-called "inverted V" fields. The FAST particle spectrum of these auroras have relatively mono-energetic peaks accompanied by an enhanced low energy component attributed to backscattered secondaries [*Evans*, 1974]. Another characteristic of this type of electron spectrum is the relatively isotropic electron pitch angle distribution. IMAGE FUV corroborated that these types of spectral features yield the most common quasi-static auroral features.

[41] During periods of this IMAGE FUV and FAST joint study we have also found the type of aurora caused by electrons characterized by field aligned pitch angle distribution and by fairly broad energy spectral enhancement [e.g., *Johnstone and Winningham*, 1982]. They are seen to form highly collimated B parallel beams and consistent with electron acceleration by wave particle interactions [*Burch*, 1991; *Temerin et al.*, 1994]. The properties of the FAST observed superthermal electrons were also similar to the features of the wave accelerated electron component obtained by simulations of the inertial Alfven waves as they propagate through an altitude dependent density profile [*Chaston et al.*, 2000].

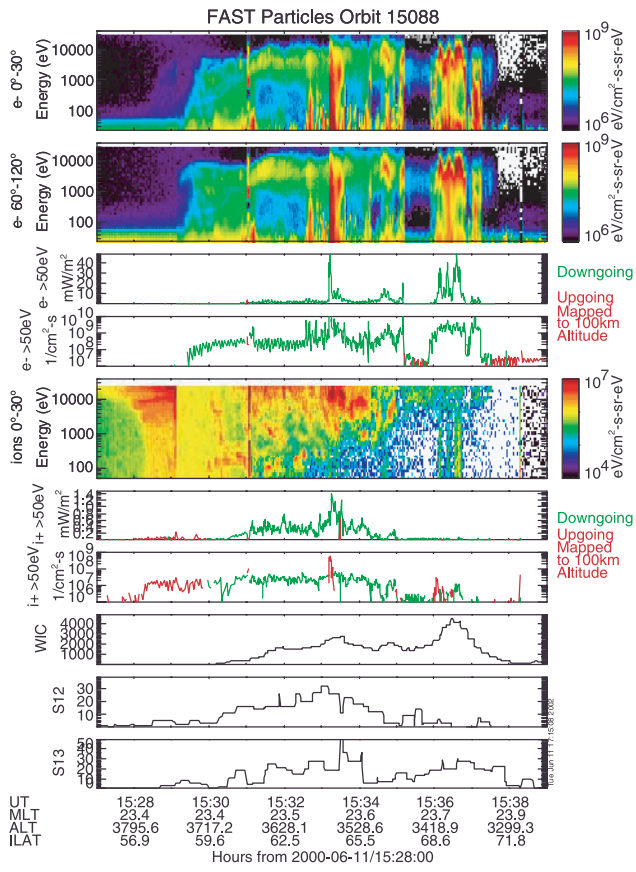

Figure 15. FAST particle and IMAGE FUV data for the orbit number 15088 (same as Figure 3).

Table 1. Selected Events With FAST Pass Within the IMAGE FUV Field of View

Date	Estimated Substorm Onset ± 3 minutes (UT)	FAST Pass Time (UT)	MLT of Pass	Remarks
10/28/2000	11:05	11:26	20.0	Intense surge superthermal electrons poleward
1/19/2002	12:49	13:49	24.0	Intense surge superthermal electrons poleward
5/12/2001	19:03	19:24	1.0	Surge west of FAST pass
5/12/2001	21:18	21:39	2.0	Surge west of FAST pass superthermal electrons in transient feature
6/11/2000	14:45	15:34	23.4	Surge west of FAST pass superthermal electrons in transient feature

[42] In Table 1 we have summarized the cases that were discussed in the paper. In two of the cases the satellite passed through an active poleward propagating surge on its duskward flank. In those cases, the superthermal wave accelerated component was found to be at the polar cap boundary of the surge. It could be cleanly isolated from inverted-V precipitation which occurred in the more equatorward parts of the auroral oval. The same signatures can be recognized in a similar DMSP spectra published by *Lopez et al.* [1991]. One can associate these auroras as the precipitation signature of the intense earthward-directed, Alfvénic wave with high Poynting fluxes observed at altitudes of 4–6 R_E near the lobe/plasma sheet interface [*Keiling et al.*, 2000; *Wygant et al.*, 2000].

[43] Thus, the active propagating substorm surge is a region where intense low energy electron precipitation [*Chaston et al.*, 2001a, 2002], coupled with intense ion outflows [*Tung et al.*, 2001], occurs. The FAST instrumentation is especially well instrumented to discriminate these regions through the high energy and pitch angle resolution of the precipitating particles.

[44] In both cases high latitude proton bursts were seen coincident with the poleward expansion by the SI-12 optical proton aurora detector. These were presumably high-energy protons that are generally out of the energy range of the satellite proton detectors.

[45] In three of the cases, FAST passed through the substorm aurora at midnight or on the dawn side outside of the surge. In these cases, we found a less clear separation of the wave accelerated electrons from the inverted V type precipitation. In two of the cases where the events were on the dawn side of the expanding surge, intense wave accelerated electrons were part of very short-lived transient events i.e., bursts.

[46] The ions were present equatorward of the surge with no enhancement poleward of their normal auroral oval position. In one of the cases, the surge was accompanied by intense ion outflow which reached about 1 keV in energy at the FAST satellite.

[47] In summary, the optical images showed that the wave accelerated superthermal electrons seen by FAST were associated with the westward part of a poleward propagating substorm surge. This region is assumed to be associated with intense Alfven waves propagating from the magnetosphere. The propagation of the surge represents a movement of the source region in the magnetosphere. We also found evidence for this type of aurora in regions dawn-ward of the surge and not necessarily at the poleward edge of the auroral oval. These were usually associated with short duration transient events. The wave acceleration suggests that the field lines in this region were undergoing some dynamic reconfiguration. Inverted V type electric field structures can be produced by steady plasma convection not requiring change in the magnetic field configuration. The IMAGE SI-13 channel has relatively high responsivity to auroras produced by high flux superthermal low energy electrons. This ability to separate the two different types of auroras by quantitative imaging raises the possibility of mapping the field lines that are connected to magnetospheric regions where magnetic field configurations are taking place.

[48] **Acknowledgments.** The IMAGE FUV instrument is a complex system involving the work of many people and a large variety of institutions. The authors would like to acknowledge the dedicated support of the staff of their respective institutions and the Southwest Research Institute (SWRI) for helping the FUV team during instrument development and satellite integration. The WIND IMF data was provided by R. Lepping of NASA/GSFC and was obtained through CDAWEB. This work was supported through SWRI subcontract number 83820 at the University of California, Berkeley, and by NASA under contract number NAS5-96020. Arthur Richmond thanks James L. Burch and another reviewer for their assistance in evaluating this paper.

References

Boehm, M. H., J. Clemmons, J.-E. Wahlund, A. Eriksson, L. Eliasson, L. Blomberg, P. Kintner, and H. Hofner, Observations of an upward-directed electron beam with the perpendicular temperature of the cold ionosphere, *Geophys. Res. Lett.*, *22*, 2103, 1995.

Burch, J. L., *Diagnosis of auroral acceleration mechanisms by particle measurements in Auroral Physics*, edited by C.-I. Meng, M. J. Rycroft, L. A. Frank, Cambridge Univ. Press, New York, 1991.

Carlson, C. W., et al., FAST observations in the downward auroral current region: energetic upgoing electron beams, parallel potential drops, and ion heating, *Geophys. Res. Lett.*, *25*, 2017, 1998.

Chaston, C. C., C. W. Carlson, R. E. Ergun, and J. P. McFadden, Alfven waves, density cavities and electron acceleration observed from the FAST spacecraft, *Phys. Scripta*, *T84*, 64–68, 2000.

Chaston, C. C., W. J. Peria, C. W. Carlson, R. E. Ergun, and J. P. McFadden, FAST observations of Inertial Alfven waves and electron acceleration in the dayside aurora, *Phys. Chem. Earth*, *26*, 201, 2001a.

Chaston, C. C., J. W. Bonnell, L. M. Peticolas, C. W. Carlson, J. P. McFadden, and R. E. Ergun, Driven Alfven waves and electron acceleration: A FAST case study, *Geophys. Res. Lett.*, *29*(11), 1535, doi:10.1029/2001GL013842, 2002.

Elphinstone, R. D., et al., The double oval UV auroral distribution, I, Implications for the mapping of auroral arcs, *J. Geophys. Res.*, *100*, 12,075, 1995a.

Elphinstone, R. D., et al., The double oval UV auroral distribution, 2, The most poleward arc system and the dynamics of the magnetotail, *J. Geophys. Res.*, *100*, 12,093, 1995b.

Ergun, R. E., et al., FAST satellite observations of electric field structures in the auroral zone, *Geophys. Res. Lett.*, *25*, 20,025, 1998.

Evans, D. S., Precipitating electron fluxes formed by a magnetic field aligned potential difference, *J. Geophys. Res.*, *79*, 2853, 1974.

Frank, L. A., and K. L. Ackerson, Observations of charged particle precipitation into the auroral zone, *J. Geophys. Res.*, *76*, 3612, 1971.

Frey, H. U., S. B. Mende, H. B. Vo, M. Brittnacher, and G. K. Parks, Conjugate observation of optical aurora with Polar satellite and ground-based cameras, *Adv. Space Res.*, *23*, 1647, 1999.

Frey, H. U., S. B. Mende, C. W. Carlson, J. C. Gérard, B. Hubert, J. Spann, R. Gladstone, and T. J. Immel, The electron and proton aurora as seen by IMAGE-FUV and FAST, *Geophys. Res. Lett.*, *28*, 1135, 2001.

Gary, J. B., L. J. Zanetti, B. J. Anderson, T. A. Potemra, J. H. Clemmons, J. D. Winningham, and J. R. Sharber, Identification of auroral oval boundaries from in situ magnetic field measurements, *J. Geophys. Res.*, *103*, 4187, 1998.

Gérard, J. C., B. Hubert, D. V. Bisikalo, V. I. Shematovich, H. U. Frey, S. B. Mende, and G. R. Gladston, Observation of the FUV proton aurora from the IMAGE satellite, *J. Geophys. Res.*, *106*, 28,939, 2001.

Hubert, B., J.-C. Gérard, D. S. Evans, M. Meurant, S. B. Mende, H. U. Frey, and T. J. Immel, Total electron and proton energy input during auroral substorms: Remote sensing with IMAGE-FUV, *J. Geophys. Res.*, *107*(A8), 10.1029/2001JA009229, 2002.

Johnstone, A. D., and J. D. Winningham, Satellite observations of suprathermal electron bursts, *J. Geophys. Res.*, *87*, 2321, 1982.

Keiling, A., J. R. Wygant, C. Cattell, M. Temerin, F. S. Mozer, C. A. Kletzing, J. Scudder, C. T. Russell, W. Lotko, and A. V. Streltsov, Large Alfven wave power in the plasma sheet boundary layer during the expansion phase of substorms, *Geophys. Res. Lett.*, *27*, 3169, 2000.

Knudsen, D. J., J. H. Clemmons, and J.-E. Wahlund, Correlation between core ion energization, suprathermal electron bursts, and broadband ELF plasma waves, *J. Geophys. Res.*, *103*, 4171, 1998.

Lopez, R. E., H. E. Spence, and C.-I. Meng, DMSP F7 observations of a substorm field-aligned current, *J. Geophys. Res.*, *96*, 19,409, 1991.

McFadden, J. P., C. W. Carlson, and R. E. Ergun, Microstructure of the auroral acceleration region as observed by FAST, *J. Geophys. Res.*, *104*, 14,453, 1999.

Mende, S. B., et al., Far ultraviolet imaging from the IMAGE spacecraft, 1, System design, *Space Sci. Rev.*, *91*, 243, 2000.

Mende, S. B., H. U. Frey, M. Lampton, J.-C. Gérards, B. Hubert, S. A. Fuselier, J. Spann, R. Gladstone, and J. L. Burch, Global observations of proton and electron auroras in a substorm, *Geophys. Res. Lett.*, *28*, 1139, 2001.

Newell, P. T., Reconsidering the inverted-V particle signature: Relative frequency of large-scale electron acceleration events, *J. Geophys. Res.*, *105*, 15,779, 2000.

Stasiewicz, K., G. Gustafsson, G. Marklund, P.-A. Lindqvist, J. Clemmons, and L. Zanetti, Cavity resonators and Alfven resonance cones observed on Freja, *J. Geophys. Res.*, *102*, 2565, 1997.

Stasiewicz, K., G. Holmgren, and L. Zanetti, Density depletions and current singularities observed by Freja, *J. Geophys. Res.*, *103*, 4251, 1998.

Stasiewicz, K., et al., Small scale alfvenic structure in the aurora, *Space Sci. Rev.*, *92*, 423–533, 2000.

Temerin, M., C. Carlson, and J. McFadden, Auroral particle acceleration, in *Proceedings of the Intenrnational Conference on Substorms-2*, edited by J. R. Kan, J. D. Craven, and S.-I. Akasofu, p. 375, Univ. of Alaska, Fairbanks, 1994.

Tung, Y.-K., C. W. Carlson, J. P. McFadden, D. M. Klumpar, G. K. Parks, W. J. Peria, and K. Liou, Auroral polar cap boundary ion conic outflow observed on FAST, *J. Geophys. Res.*, *106*, 3603, 2001.

Wahlund, J.-E., et al., Broadband ELF plasma emission during auroral energization, 1, Slow ion acoustic waves, *J. Geophys. Res.*, *103*, 4343, 1998.

Wygant, J. R., et al., Polar spacecraft based comparisons of intense electric fields and Poynting flux near and within the plasma sheet-tail lobe boundary to UVI images: An energy source for the aurora, *J. Geophys. Res.*, *105*, 18,675, 2000.

C. W. Carlson, H. U. Frey, T. J. Immel, and S. B. Mende, Space Sciences Laboratory, University of California, Centennial Drive at Grizzly Peak Blvd., Berkeley, CA 94720, USA. (mende@ssl.berkeley.edu)

J.-C. Gérard, Laboratoire de Physique Atmosphérique et Planétaire, Institut d'Astrophysique, L'Université de Liège, Belgium.